NANO LETTERS

pubs.acs.org/NanoLett

Letter

# *N*-Terminal Lysozyme Conjugation to a Cationic Polymer Enhances Antimicrobial Activity and Overcomes Antimicrobial Resistance

Tong Zhang,[†] Wei An,[†] Jiawei Sun, Fei Duan, Zeyu Shao, Fan Zhang, Ting Jiang,* Xuliang Deng,* Cyrille Boyer,* and Weiping Gao*

Cite This: *Nano Lett.* 2022, 22, 8294–8303

Read Online

ACCESS | Metrics & More | Article Recommendations | Supporting Information

**ABSTRACT:** Microbial resistance to antibiotics is one of the greatest global healthcare challenges. There is an urgent need to develop effective strategies to overcome antimicrobial resistance. We, herein, report photoinduced in situ growth of a cationic polymer from the *N*-terminus of lysozyme. The attachment of the cationic polymer improves the proteolytic and thermal stability of lysozyme. Notably, the conjugate can efficiently overcome lysozyme resistance in Gram-positive bacteria and antibiotics-resistance in Gram-negative bacteria, which may be ascribed to the synergistic interactions of lysozyme and the cationic polymer with the bacteria to disrupt their cell membranes. In a rat periodontitis model, the lysozyme-polymer conjugate not only greatly outperforms lysozyme in therapeutic efficacy but also is superior to minocycline hydrochloride, which is the gold standard for periodontitis therapy. These findings may provide an efficient strategy to dramatically enhance the antimicrobial activities of lysozyme and pave a way to overcome antimicrobial resistance.

**KEYWORDS:** *protein−polymer conjugate, lysozyme, protein delivery, antimicrobial, antimicrobial resistance*

Downloaded via PEKING UNIV on February 6, 2023 at 01:31:31 (UTC).
See https://pubs.acs.org/sharingguidelines for options on how to legitimately share published articles.

Antimicrobial resistance is now a pressing global healthcare issue due to the overuse of antibiotics.[1,2] To combat this global challenge, the development of novel antibiotic agents or effective therapeutic strategies is urgently needed. Antimicrobial peptides or proteins (AMPs) are ubiquitous in nature and play a key role in the innate immunity of an organism.[3−7] They can kill pathogenic microbes and sometimes cancerous cells. AMPs are typically positively charged and amphiphilic, allowing for semiselective binding to negatively charged bacterial cells during insertion into and disruption of the bacterial cell membrane. Recent studies demonstrate that AMPs disrupt various key cellular processes to achieve their antimicrobial activity.[8,9] These antimicrobial characteristics of AMPs make microbes less likely to develop resistance, which is distinct from antibiotics that microbes can adapt by gene mutation to become resistant.[10−12]

Lysozyme (LYS) is an important AMP, which is widely distributed in immune cells and body fluids.[13] LYS catalytically hydrolyzes $\beta$-1,4-glycosidic bonds between *N*-acetyl muramic acid and *N*-acetylglucosamine that are alternating units in the peptidoglycan layer of the bacterial cell wall, leading to the lysis of the bacteria to death. LYS is active in killing Gram-positive bacteria, whereas it is less effective in killing Gram-negative bacteria. Additionally, several pathogenic bacteria have developed mechanisms to evade LYS-catalyzed killing.[14] Recently, LYS has been immobilized onto nanoparticles based on organic and inorganic materials to improve its stability.[15−17] However, the improvement in stability was typically accompanied by a decrease in antimicrobial activity due to the nonspecific immobilization of LYS on the surfaces of these nanoparticles.

To enhance the antimicrobial activity and stability of LYS and to overcome the antimicrobial resistance, we report photoinduced in situ growth of poly(*N,N*′-dimethylamino-2-ethyl methacrylate) (PDMAEMA) at the *N*-terminus of LYS to form an *N*-terminal LYS-PDMAEMA conjugate (Figure 1a). We chose to modify LYS at the *N*-terminus, as this group is not the site of bioactivity.[18,19] A hydroxylamine-functional atom transfer radical polymerization (ATRP) initiator, (2-(aminooxy)ethyl) 2-bromo-2-methylpropanoate (ABM), was specifically synthesized and attached to the *N*-terminus in the presence of 2,6-pyridinedicarboxaldehyde (PDA). The cationic polymer of PDMAEMA was directly grown from the resulting LYS-based ATRP initiator (LYS-Br), via photoinduced ATRP, to form a LYS-PDMAEMA conjugate without significantly affecting LYS's enzymatic activity. The conjugate not only increased the stability of LYS but also greatly improved its

**Received:** August 9, 2022
**Revised:** October 11, 2022
**Published:** October 14, 2022

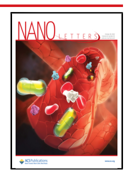

ACS Publications © 2022 American Chemical Society



https://doi.org/10.1021/acs.nanolett.2c03160
*Nano Lett.* 2022, 22, 8294–8303

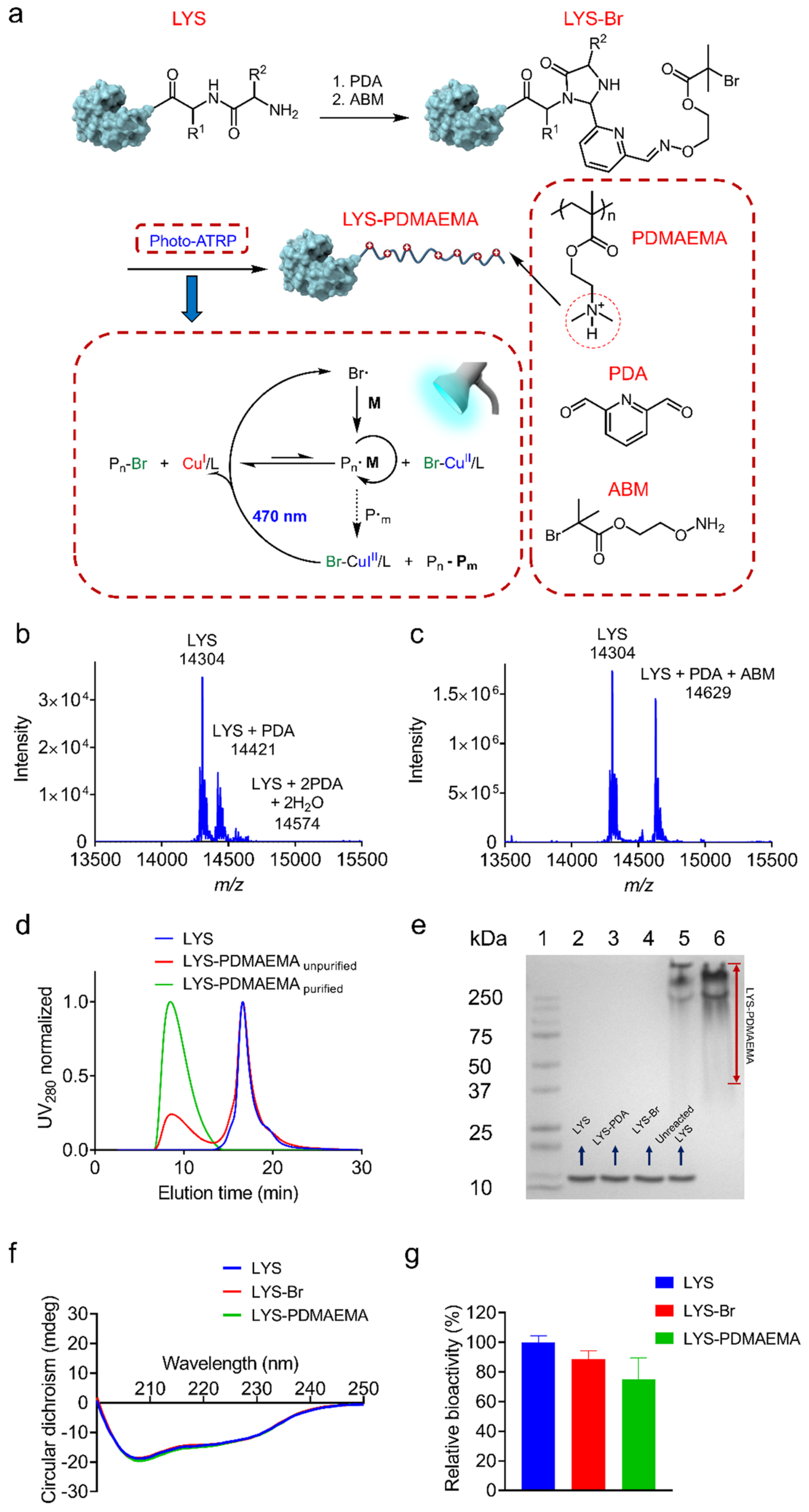


**Figure 1.** Synthesis of LYS-PDMAEMA. (a) Scheme of the synthesis of LYS-PDMAEMA via PDA-mediated *N*-terminal modification and photoinduced ATRP. (b) Q-TOF-MS of LYS-PDA. (c) Q-TOF-MS of LYS-Br. (d) GPC traces of LYS, LYS-Br, unpurified LYS-PDMAEMA, and purified LYS-PDMAEMA (e) Gel electrophoresis analysis of the synthesis of LYS-PDMAEMA: lane 1, marker; lane 2, LYS; lane 3, LYS-PDA; lane 4, LYS-Br; lane 5, unpurified LYS-PDMAEMA; lane 6, purified LYS-PDMAEMA. (f) CD spectra of LYS, LYS-Br, and LYS-PDMAEMA. (g) Enzymatic activity of LYS, LYS-Br, or LYS-PDMAEMA. Note: The protein structure in part a was generated from PDB ID 1LYZ,[29] created with ChimeraX.[30]



https://doi.org/10.1021/acs.nanolett.2c03160
Nano Lett. 2022, 22, 8294−8303

antibacterial activity against LYS-resistant Gram-positive bacteria. More importantly, the LYS-PDMAEMA conjugate exhibited an excellent activity against Gram-negative bacteria and antibiotic-resistant Gram-negative bacteria, whereas LYS alone showed a very low activity against Gram-negative bacteria. The antimicrobial activity of the conjugate was confirmed in vivo using a rat periodontitis model. The conjugate exhibited enhanced therapeutic efficacy over LYS and superior efficacy to minocycline hydrochloride, which is the most widely used antibiotic for periodontitis therapy.

*N*-Terminal modification is one of the most frequently used site-selective protein modifications because of the unique structure of the *N*-terminus.[20−23] Pyridoxal-5′-phosphate (PLP)-mediated transamination is the extensively used method for *N*-terminal modification[24−26] However, this method suffers from low transamination efficiency when the *N*-terminal amino acid residue is lysine, histidine, isoleucine, glutamine, tryptophan, or proline.[21,22] Unfortunately, we found less than 10% conversion for the PLP-mediated *N*-terminal modification of LYS. This is because the *N*-terminal amino acid residue of LYS is lysine.[27] Alternatively, our group has recently developed a general and efficient method of PDA-mediated *N*-terminal modification.[28] Therefore, we turned to this method to modify the *N*-terminal end of LYS.

To conjugate the ATRP initiator of ABM to the *N*-terminus of LYS, LYS was first reacted with PDA to form LYS-PDA through imidazolidinone formation (Figure 1a). After the reaction, a significant portion of LYS + PDA (14,421 Da) and a small portion of LYS + 2PDA + $2H_2O$ (14,574 Da) were observed by quadrupole time-of-flight mass spectrometry (Q-TOF-MS) (Figure 1b), indicating the formation of the adducts of LYS and PDA. After chymotrypsin digestion of the product mixture, the resultant peptide fragments were analyzed by liquid chromatography-tandem mass spectrometry (LC-MS/MS). We detected only the peptide fragment of PDA-KVFGRCELAA at the *N*-terminus (Figure S1), indicating the exclusive formation of the cyclic imidazolidinone at the *N*-terminus. Next, the mixture was reacted with ABM to produce LYS-Br through oxime formation between the hydroxylamine group of ABM and the pending aldehyde group of the cyclic imidazolidinone at the *N*-terminus. The formation of LYS-PDA-ABM (LYS-Br,14,629 Da) was verified by Q-TOF-MS (Figure 1c). Moreover, only the peptide fragment of ABM-KVFGRCEL functionalized at the *N*-terminus was found after chymotrypsin digestion of the product (Figure S2). These results indicate the selective modification of the initiator at the *N*-terminus of LYS.

Visible light-initiated photo-ATRP can be performed at room temperature and without the need of deoxygenation. Furthermore, the reaction can be easily controlled by turning light on and off.[31−34] These characteristics are especially beneficial for the preparation of protein-polymer conjugates. To evidence that the antimicrobial activity of LYS is not affected by exposure to visible light, we exposed LYS to blue light irradiation ($\lambda_{max}$ = 450 nm) at 25 °C for 4 h. After blue light exposure, the enzymatic activity of LYS against *Micrococcus lysodeikticus* was found to be unchanged (Figure S3a). Motivated by this favorable result, we further tested our photo-ATRP system using DMAEMA as the monomer and LYS-Br as the initiator. After the photoinduced ATRP reaction, the solution was directly examined by aqueous gel permeation chromatography (GPC) (Figure 1d). A new peak appeared at a lower retention time relative to the peak of LYS-Br, which is attributed to the formation of the LYS-PDMAEMA conjugate. Additionally, the unreacted LYS-Br residue, including some unmodified LYS, was removed via cationic exchange chromatography. After the purification, the unimodal GPC peak corresponding to LYS-PDMAEMA was observed, indicating success in the purification. These results were further supported by gel electrophoresis (Figure 1e). A smear for a LYS-PDMAEMA conjugate was observed at the high molecular weight region with the presence of unreacted LYS at the low molecular weight region (lane 6). The band for the residual LYS and LYS-Br disappeared (lane 7) after the purification, indicating the success of purification. A smear for the conjugate was observed after the reaction and the band for the residual LYS and LYS-Br disappeared after the purification. The smearing of the LYS-PDMAEMA conjugate on the gel was possibly caused by the interaction between the cationic polymer and the polyacrylamide gel. After digestion with proteinase K to remove LYS from the conjugate, GPC was used to determine the number-averaged molecular weight and dispersity of the PDMAEMA residue to be 16.4 kDa and 1.35, respectively (Figure S4b). The chemical structure of PDMAEMA was also identified by proton nuclear magnetic resonance ($^1$H NMR) (Figure S4c). Circular dichroism showed the almost identical traces of native LYS, LYS-Br, and LYS-PDMAEMA (Figure 1f), indicating the intact retention of the secondary structure of LYS after the two-step *N*-terminal reactions. The enzymatic activities of LYS-Br and LYS-PDMAEMA against the substrate of lyophilized *Micrococcus lysodeikticus* were determined to be 89% and 75% of LYS (Figure 1g), indicating the slight reduction of enzymatic activity after the *N*-terminal modifications. In contrast, nonspecific modification of LYS with ATRP initiators at the lysine residues led to 19% of its original enzymatic activity (Figure S3b). These results indicate the importance of the selective *N*-terminal modification in the retention of LYS's bioactivity. This is because the *N*-terminus is far away from the active site residue 52.[35]

Next, we investigated the thermal and proteolytic stability of LYS-PDMAEMA and LYS. After incubation at 90 °C, as expected, LYS rapidly lost 97% of its original enzymatic activity within 30 min, whereas LYS-PDMAEMA retained 40% of its original enzymatic activity (Figure 2a), indicating the enhanced thermal stability of LYS-PDMAEMA over LYS. After incubation with proteinase K at 37 °C, LYS completely lost its activity within 12 h, whereas LYS-PDMAEMA retained 37% of its original activity (Figure 2b), indicating the significantly improved proteolytic stability of LYS-PDMAEMA over LYS due to the physical shielding of the conjugated polymer on the lysozyme surface. The polymer conjugation of protein typically results in better thermal, proteolytic, and storage stability.[36] Similar phenomena were observed in the cases of protein-polymer conjugates in the literature.[25,37,38] Overall, these results demonstrate that the *N*-terminal PDMAEMA conjugation can considerably improve the thermal and proteolytic stability of LYS.

After having demonstrated the successful preparation of the LYS-PDMAEMA conjugate, we investigated the antibacterial activities of LYS-PDMAEMA and LYS against Gram-positive bacteria of *M. lysodeikticus* and Gram-negative bacteria of *E. coli*. At a fixed LYS concentration of 10 $\mu$M, LYS exhibited an excellent antimicrobial efficiency against *M. lysodeikticus* (Figure 3a) but a much low antibacterial efficiency against *E. coli* (Figure 3b). In contrast, LYS-PDMAEMA was found to


https://doi.org/10.1021/acs.nanolett.2c03160
Nano Lett. 2022, 22, 8294−8303

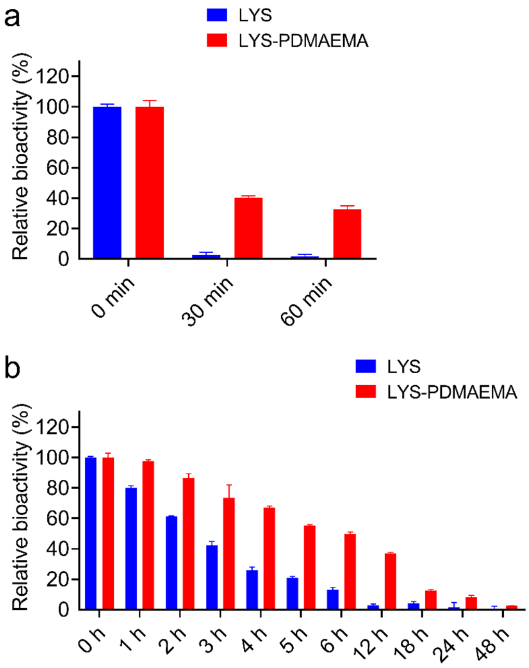


**Figure 2.** Thermal and enzymatic stability of LYS and LYS-PDMAEMA. (a) Bioactivity of LYS and LYS-PDMAEMA after incubation at 90 °C. (b) Bioactivity of LYS and LYS-PDMAEMA after incubation with proteinase K.

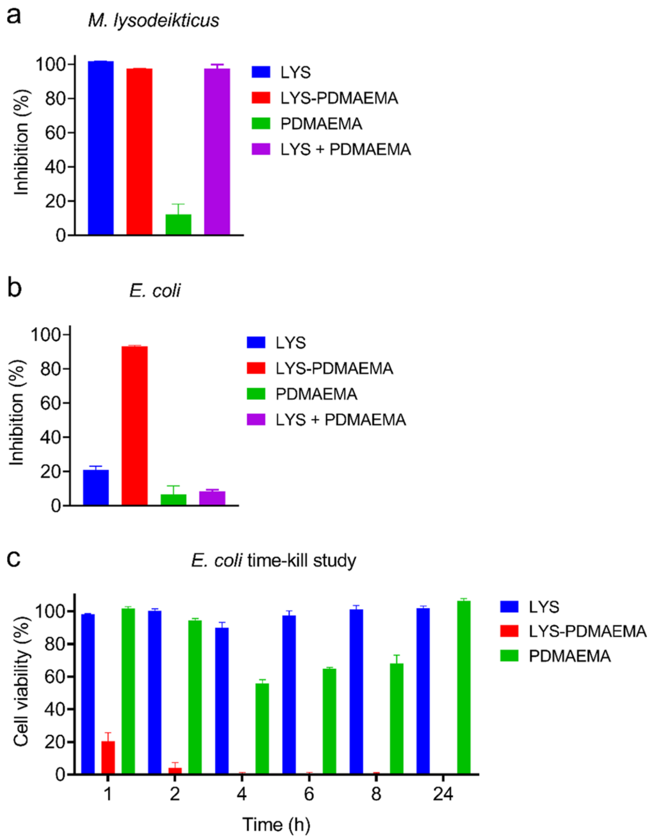


**Figure 3.** Antimicrobial activity of LYS-PDMAEMA against Gram-positive or Gram-negative bacteria. (a, b) Preliminary study of inhibition of *M. lysodeikticus* and *E. coli* growth by LYS, LYS-PDMAEMA, PDMAEMA, and the physical mixture of LYS and PDMAEMA (LYS + PDMAEMA) at a fixed concentration of LYS = 10 $\mu$M. (c) Time-kill study for LYS, LYS-PDMAEMA, and PDMAEMA against *E. coli*.

not only be as efficient as LYS in inhibiting *M. lysodeikticus* growth, but it was also much more efficient than LYS in inhibiting *E. coli* growth. Additionally, PDMAEMA was much less effective than both LYS-PDMAEMA and LYS in inhibition of growth of both bacteria. Furthermore, the physical combination of LYS and PDMAEMA showed an activity similar to LYS against *M. lysodeikticus* or to PDMAEMA against *E. coli*. Specifically, LYS-PDMAEMA could completely kill *E. coli* within 4 h, whereas LYS was not effective in killing *E. coli* even after 24 h of incubation (Figure 3c). These results were further verified by the optical images of the bacteria solutions (Figure S5). The solution of *E. coli* after incubation with LYS-PDMAEMA was clear and transparent, indicating that the bacteria were killed by the conjugate. In contrast, the solutions of *E. coli* treated with LYS and PDMAEMA looked turbid, indicating the poor antibacterial property of LYS and PDMAEMA. Notably, PDMAEMA inhibited *E. coli* growth to some degree for a short period of 4 h, but the bacteria could grow over a more extended incubation period (Figure 3c). This wave-like inhibition kinetics could be attributed to the poor bactericidal property of the polycation PDMAEMA. Over a shorter incubation period, this cationic polymer can inhibit the growth of Gram-negative bacteria; however, the bacteria could grow back over a longer period. Similar phenomena were observed in the cases of cationic polymers in the literature.[39] These results demonstrate that the attachment of PDMAEMA can significantly enhance the antibacterial activity of LYS against Gram-negative bacteria.

We further quantified the antibacterial activities of LYS-PDMAEMA and LYS against Gram-positive bacteria (*M. lysodeikticus* and *S. mutans*) and Gram-negative bacteria (*E. coli*, antibiotic-resistant *E. coli*, and *P. gingivalis*) by determining the values of minimum bactericidal concentration (MBC) and minimum inhibitory concentration (MIC) (Tables 1 and S1). As expected, both the MBC and MIC values of the LYS-PDMAEMA conjugate against Gram-negative bacteria are 1 or 2 orders of magnitude lower than those of LYS, indicating the considerably enhanced antibacterial activity of LYS-PDMAEMA over LYS against Gram-negative bacteria and antibiotic-resistant Gram-negative bacteria. Both the MBC and MIC values of LYS-PDMAEMA against *M. lysodeikticus* are a few times higher than those of LYS, indicating the slightly reduced antibacterial activity against Gram-positive bacteria of LYS-PDMAEMA over LYS. However, both the MBC and MIC values of LYS-PDMAEMA against LYS-resistant Gram-positive bacteria *S. mutans* are 2 orders of magnitude lower than those of LYS, indicating the dramatically enhanced antibacterial activity against LYS-resistant Gram-positive bacteria of LYS-PDMAEMA over LYS. Together, all of these results demonstrate that the *N*-terminal LYS conjugation to PDMAEMA greatly enhances the antibacterial activity against both Gram-negative and antibiotic-resistant Gram-negative bacteria and LYS-resistant Gram-positive bacteria.

To investigate the antibacterial mechanism of the LYS-PDMAEMA conjugate, the conjugate was labeled with the fluorophore Cy5 to evaluate the interaction between the conjugate and bacteria by confocal laser scanning microscopy (CLSM) (Figure 4a). Gram-negative bacteria of *E. coli* were selected for the antimicrobial mechanism study. The Cy5-labeled LYS-PDMAEMA conjugate was incubated with bacteria for 30 min, and then the bacteria were separated

**Table 1. MIC and MBC Values of LYS and LYS-PDMAEMA against Various Bacteria**

| | MIC ($\mu$g mL$^{-1}$) | | | | |
|---|---|---|---|---|---|
| | *M. lysodeikticus* | *E. coli* | *E. coli* *[a] | *S. mutans* | *P. gingivalis* |
| LYS | 0.015 | >10000 | >10000 | >10000 | 3125 |
| LYS-PDMAEMA | 0.07 | 120 | 200 | 250 | 250 |
| | MBC ($\mu$g mL$^{-1}$) | | | | |
| | *M. lysodeikticus* | *E. coli* | *E. coli* *[a] | *S. mutans* | *P. gingivalis* |
| LYS | 0.03 | >10000 | >10000 | >10000 | 6250 |
| LYS-PDMAEMA | 0.15 | 240 | 500 | 250 | 500 |

[a]*E. coli** with chloramphenicol resistance gene.

from the media by centrifugation and washed. A strong red fluorescence was observed on and inside the bacterial cells, indicating that the conjugate can strongly interact with the *E. coli* membrane and then enter the inside of the bacteria. In contrast, LYS cannot interact with the bacteria, as indicated by no red fluorescence observed on or inside the bacteria after incubation with Cy5-labeled LYS. These phenomena were also found in the case of *P. gingivalis* (Figure S6). Additionally, the adsorption of PDMAEMA on the membrane of bacteria was reported in the literature.[39] Therefore, the strong interaction of LYS-PDMAEMA with the bacteria could be ascribed to the multivalent electrostatic interaction of the positively charged PDMAEMA with the negatively charged membranes of the bacteria.

Due to the resolution limitation of CLSM, it is difficult to observe the detailed action of Cy5-labeled LYS-PDMAEMA in the bacteria membrane region. Thus, we utilized scanning electron microscopy (SEM) for further investigation on the disruption of the bacteria membrane. A significant morphology change was observed for LYS-PDMAEMA-treated *E. coli* (Figure 4b). A rod shape with an integrated surface was observed for *E. coli* treated with LYS, indicating LYS cannot disrupt the cell membrane and change the cell morphology. In contrast, an obvious change in the cell membrane morphology of *E. coli* treated with the conjugate was observed and some cells were fragmented after a 1 h incubation. Similar phenomena were also observed in the case of *P. gingivalis and S. mutans* (Figure S7). These results indicate that the conjugate exerts a strong bactericidal activity through membrane disruption. To confirm the mechanism of membrane disruption, membrane potential measurements were performed to determine the ability of the LYS-PDMAEMA conjugate to disturb the membrane of *E. coli.* A carbocyanine dye, 3,3′-diethyloxacarbocyanine iodide [DiOC$_2$(3)], was employed in this experiment following the procedures in the literature.[40] DiOC$_2$(3) exhibits red fluorescence with the accumulation in bacteria cytosol, but as the bacteria lose membrane potential, the intensity decreases and shifts to green fluorescence (due to disruption events).[41] The red fluorescence (670 nm emission) intensity was recorded to measure the loss in membrane potential that corresponds to the degree of membrane disruption. As shown in Figure S8, after a 5 min incubation, the LYS- or PDMAEMA-treated bacteria cells presented almost 100% red fluorescence intensity compared to the original, indicating no disruption of the membrane region. In contrast, *E. coli* cells exhibited a loss in membrane potential at a high concentration (>250 $\mu$g/mL) after incubation with LYS-PDMAEMA for 5 min, suggesting that the LYS-PDMAEMA conjugate is capable of disrupting the bacteria membrane.

On the basis of these results, we attributed the membrane disruption to the synergy of the electrostatic interaction of the positively charged PDMAEMA with the negatively charged cell membranes and the hydrolytic activity of LYS (Figure 4c).

The cytotoxicity of LYS-PDMAEMA and LYS was evaluated by hemolysis using red blood cells (RBCs) and cell viability using 3T3 fibroblast cell. The hemolytic activity of the LYS analogues was determined by testing the hemoglobin release from RBCs into the supernatant. Less than 5% red blood cell hemolysis ratios were observed for all the tested LYS analogues over a wide range of concentrations (Figure S9), which indicates the excellent RBC compatibility. As expected, the 3T3 cell viability of LYS-PDMAEMA was found lower than that of LYS, especially at high concentrations (Figure S10), indicating that LYS-PDMAEMA is more cytotoxic than LYS at high concentrations. However, LYS-PDMAEMA was found to be much less cytotoxic than PDMAEMA at high concentrations, indicating the incorporation of LYS can reduce the cytotoxicity of PDMAEMA.

Over 700 species of microorganisms live in the human oral cavity.[42,43] Generally, bacteria living in the oral cavity maintain the balance between the flora and the host in a complex symbiotic way, which is significant in maintaining oral health.[44−47] Periodontal disease occurs when the periodontal microorganism loses balance with the host and becomes dysbiosis.[48] Periodontitis is a chronic infectious disease caused by microorganisms in dental plaque.[49] Tooth loosening and extraction[50] would occur due to the long-term inflammation and expansion to the deep periodontal supporting tissue, followed by the destruction of these tissues. Periodontitis has become the number one cause of tooth loss in adults.[51] Periodontitis is a multifactor disease caused by microorganism infection and poor dental hygiene. Moreover, dental plaque microbes are the initiating factor that causes inflammation and destruction of periodontal tissues. The bacteria that cause periodontitis are mainly Gram-negative anaerobic bacteria, including *P. gingivalis*, *F. nucleatum*, *T. forsythia*, and *A. actinomycetemcomitans*.[52]

For the treatment of periodontitis, the most commonly used clinical treatments include mechanical therapy and the synergy of mechanical and drug adjuvant therapy. However, due to anatomical factors and the problem of antibiotic resistance, some cases with deep and complicated periodontal pockets often have a limited therapeutic effect and lack efficient removal of plaque microorganisms.[53] Therefore, developing a novel antimicrobial material with excellent antibacterial properties and against drug resistance becomes an urgent need.

To further investigate the antibacterial activity of the LYS-PDMAEMA conjugate in vivo, we selected a rat periodontitis model that was established by silk ligation and oral inoculation


https://doi.org/10.1021/acs.nanolett.2c03160
*Nano Lett.* 2022, 22, 8294−8303

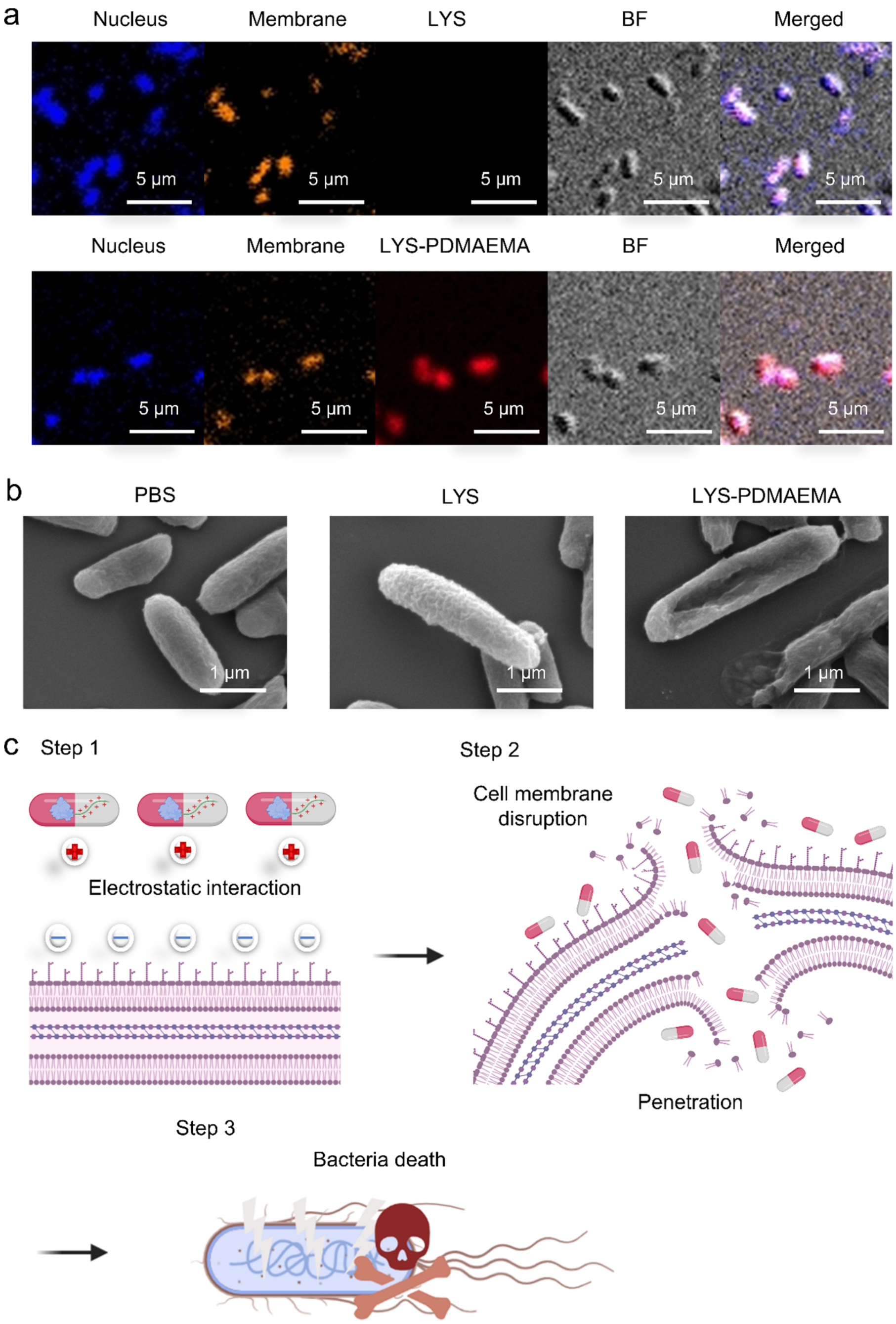


**Figure 4.** Antibacterial mechanism study of LYS-PDMAEMA. (a) CLSM images of *E. coli* incubated with Cy5-labeled LYS and LYS-PDMAEMA (red). The nucleus was stained with DAPI (blue). The membrane was stained with Dil (yellow). (b) SEM images of *E. coli* treated with LYS and LYS-PDMAEMA. (c) Scheme of the antibacterial mechanism of LYS-PDMAEMA. First, the conjugate adsorbs on the surface of bacteria due to the strong electrostatic interaction between them. Second, LYS catalyzes the hydrolysis of the peptidoglycan layer of the bacterial cell wall. The conjugate disrupts the cell membranes and gets into the inside of the cell. Finally, the bacterial cell is killed. Note: Part c was created with BioRender.com.

with *P. gingivalis*. As a control, we used minocycline hydrochloride as antibiotic, which is commonly employed for the treatment of periodontitis. A microcomputed tomography (CT) scan was performed on the upper left second molar of the rat and its surrounding area after the treatments with antibiotic, LYS, or LYS-PDMAEMA (Figures 5a and S11). The different distances from the cementoenamel junction (CEJ, blue line) to the alveolar bone crest (ABC, yellow line) indicate varying degrees of bone loss (Figure 5b). As expected, without treatment with antibiotic or LYS-PDMAEMA, periodontitis resulted in severe alveolar bone loss (ABL, red arrow). We found that LYS-PDMAEMA was equal to minocycline hydrochloride but much more efficient than LYS in reducing bone loss. As expected, without treatment with antibiotic or LYS-PDMAEMA, periodontitis resulted in severe bone resorption. We found that LYS-PDMAEMA was equal to minocycline hydrochloride but much more efficient than LYS in reducing bone resorption. In contrast, LYS was almost ineffective in this aspect. Quantification of micro-CT data showed that periodontitis caused significant reductions in bone


https://doi.org/10.1021/acs.nanolett.2c03160
*Nano Lett.* 2022, 22, 8294−8303

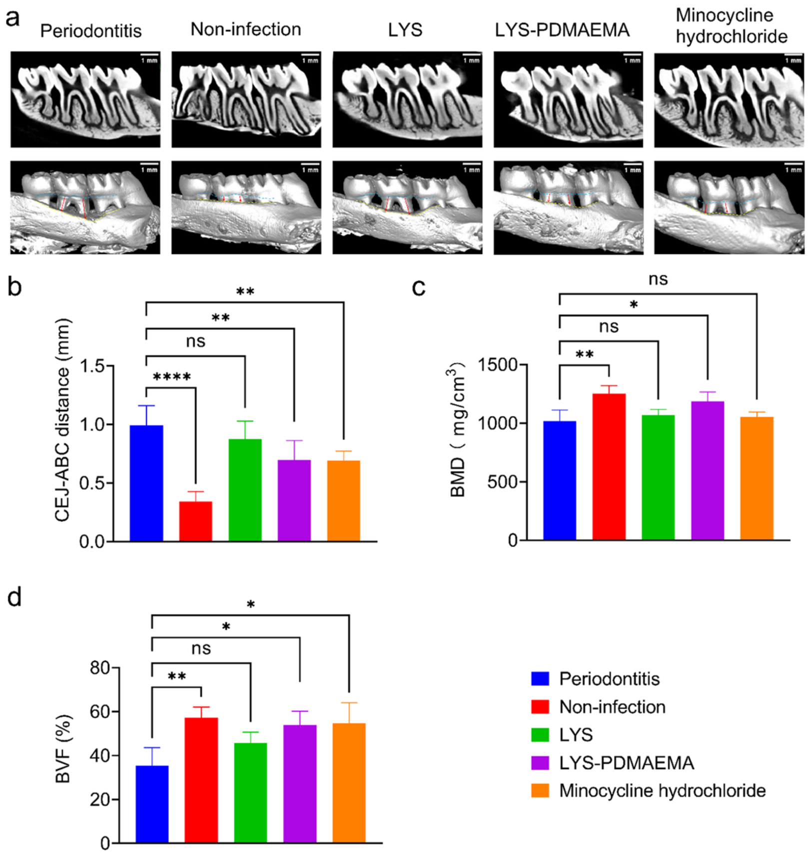


**Figure 5.** Anti-periodontitis efficacy of LYS-PDMAEMA in a rat model of *P. gingivalis* infection. (a) Micro-CT images after the treatments: blue line, cemento-enamel junction (CEJ); yellow line, alveolar bone crest (ABC); red line, alveolar bone loss (ABL). (b) CEJ-ABC distances after the treatments. (c) BMDs after the treatments. (d) BVFs after the treatments. *Statistically significant with respect to the control according to One Way ANOVA; $n = 3$, $^{*}p < 0.05$, $^{**}p < 0.01$, $^{***}p < 0.001$, $^{****}p < 0.0001$.

mineral density (BMD) and bone volume fraction (BVF, BV/TV) (Figure 5c, d). However, we observed minimal change in the BMD and BVF after the LYS-PDMAEMA treatment, whereas LYS was ineffective and was similar to the untreated controls. Although the minocycline hydrochloride treatment was similar to the LYS-PDMAEMA treatment in bone fraction volume (BVF, Figure 5d), it led to a lower BMD than LYS-PDMAEMA (Figure 5c), indicating less damage of LYS-PDMAEMA to the bone structure compared with the antibiotic. In addition, LYS-PDMAEMA has a better capability against drug-resistant development than antibiotics. These results indicate that LYS-PDMAEMA is not only much more efficient than LYS but also slightly better than minocycline hydrochloride in periodontitis therapy.

In summary, the unique methods of PDA-mediated *N*-terminal modification and photoinduced in situ ATRP make it possible to specifically and efficiently conjugate the cationic polymer PDMAEMA to the *N*-terminus of LYS. The LYS-PDMAEMA conjugate not only well retains the hydrolytic activity of LYS but also significantly improves the proteolytic and thermal stability of LYS, indicating the importance of the *N*-terminal LYS conjugation to PDMAEMA in bioactivity retention and stability improvement. Notably, the conjugate drastically enhances the antibacterial activity of LYS against both Gram-negative bacteria and antibiotic-resistant Gram-negative bacteria. More interestingly, it can overcome the LYS resistance in Gram-positive bacteria. These advantages of the conjugate over LYS make it promising as a novel general non-antibiotic drug for the treatment of infectious disease. We ascribe these attributes of the conjugate to the synergistic interactions of the positively charged PDMAEMA and the enzymatically active LYS of the conjugate with the bacteria to disrupt the cell membranes. On the basis of the proposed mechanism, we imagine that more novel non-antibiotic drugs would be developed in the future. Additionally, our in vivo data demonstrate that the conjugate dramatically outperforms LYS and even is superior to the gold standard minocycline hydrochloride in the treatment of periodontitis in a rat model. These findings indicate the potential of the conjugate as an alternative to minocycline hydrochloride in periodontitis therapy.

## ■ ASSOCIATED CONTENT

### Supporting Information

The Supporting Information is available free of charge at https://pubs.acs.org/doi/10.1021/acs.nanolett.2c03160.

> Materials; experimental details; and supplementary results including LC/MS spectra, MS/MS spectra, bioactivity measurements, mass spectrometry, gel permeation chromatography (GPC), $^{1}$H NMR, MIC and MBC values, CLSM images, SEM images, membrane potential measurements, hemolysis study, cell viability, and Micro-CT images. (PDF)


https://doi.org/10.1021/acs.nanolett.2c03160
Nano Lett. 2022, 22, 8294−8303

## AUTHOR INFORMATION


### Corresponding Authors

**Ting Jiang** − *Department of Prosthodontics, Peking University School and Hospital of Stomatology & National Center of Stomatology & National Clinical Research Center for Oral Diseases & National Engineering Research Center of Oral Biomaterials and Digital Medical Devices & Beijing Key Laboratory of Digital Stomatology & Research Center of Engineering and Technology for Computerized Dentistry Ministry of Health & NMPA Key Laboratory for Dental Materials, Beijing 100081, China*; Email: jt_ketizu@163.com

**Xuliang Deng** − *Department of Geriatric Dentistry, Beijing Laboratory of Biomedical Materials, Peking University School and Hospital of Stomatology, Beijing 100081, China; Biomedical Engineering Department, Peking University, Beijing 100191, China; Peking University-Yunnan Baiyao International Medical Research Center, Beijing 100191, China*; Email: kqdengxuliang@bjmu.edu.cn

**Cyrille Boyer** − *Centre for Advanced Macromolecular Design and Australian Centre for NanoMedicine, School of Chemical Engineering, The University of New South Wales, Sydney, NSW 2052, Australia*; orcid.org/0000-0002-4564-4702; Email: cboyer@unsw.edu.au

**Weiping Gao** − *Department of Geriatric Dentistry, Beijing Laboratory of Biomedical Materials, Peking University School and Hospital of Stomatology, Beijing 100081, China; Biomedical Engineering Department, Peking University, Beijing 100191, China; Institute of Medical Technology, Health Science Center of Peking University, Beijing 100191, China; Peking University International Cancer Institute, Beijing 100191, China; Peking University-Yunnan Baiyao International Medical Research Center, Beijing 100191, China*; orcid.org/0000-0002-2916-3044; Email: gaoweiping@hsc.pku.edu.cn

### Authors

**Tong Zhang** − *Department of Prosthodontics, Peking University School and Hospital of Stomatology & National Center of Stomatology & National Clinical Research Center for Oral Diseases & National Engineering Research Center of Oral Biomaterials and Digital Medical Devices & Beijing Key Laboratory of Digital Stomatology & Research Center of Engineering and Technology for Computerized Dentistry Ministry of Health & NMPA Key Laboratory for Dental Materials, Beijing 100081, China; Department of Geriatric Dentistry, Beijing Laboratory of Biomedical Materials, Peking University School and Hospital of Stomatology, Beijing 100081, China; Biomedical Engineering Department, Peking University, Beijing 100191, China; Centre for Advanced Macromolecular Design and Australian Centre for NanoMedicine, School of Chemical Engineering, The University of New South Wales, Sydney, NSW 2052, Australia*

**Wei An** − *Department of Prosthodontics, Peking University School and Hospital of Stomatology & National Center of Stomatology & National Clinical Research Center for Oral Diseases & National Engineering Research Center of Oral Biomaterials and Digital Medical Devices & Beijing Key Laboratory of Digital Stomatology & Research Center of Engineering and Technology for Computerized Dentistry Ministry of Health & NMPA Key Laboratory for Dental Materials, Beijing 100081, China*

**Jiawei Sun** − *Department of Geriatric Dentistry, Beijing Laboratory of Biomedical Materials, Peking University School and Hospital of Stomatology, Beijing 100081, China; Biomedical Engineering Department, Peking University, Beijing 100191, China; Institute of Medical Technology, Health Science Center of Peking University, Beijing 100191, China; Peking University International Cancer Institute, Beijing 100191, China; Peking University-Yunnan Baiyao International Medical Research Center, Beijing 100191, China*

**Fei Duan** − *Department of Geriatric Dentistry, Beijing Laboratory of Biomedical Materials, Peking University School and Hospital of Stomatology, Beijing 100081, China; Biomedical Engineering Department, Peking University, Beijing 100191, China; Peking University International Cancer Institute, Beijing 100191, China; Peking University-Yunnan Baiyao International Medical Research Center, Beijing 100191, China*

**Zeyu Shao** − *Centre for Advanced Macromolecular Design and Australian Centre for NanoMedicine, School of Chemical Engineering, The University of New South Wales, Sydney, NSW 2052, Australia*

**Fan Zhang** − *Department of Geriatric Dentistry, Beijing Laboratory of Biomedical Materials, Peking University School and Hospital of Stomatology, Beijing 100081, China; Biomedical Engineering Department, Peking University, Beijing 100191, China; Peking University International Cancer Institute, Beijing 100191, China; Peking University-Yunnan Baiyao International Medical Research Center, Beijing 100191, China*

Complete contact information is available at: https://pubs.acs.org/10.1021/acs.nanolett.2c03160


### Author Contributions

[†]T.Z. and W.A contributed equally to this work. W.G. conceived the project. T.Z., W.A., J.S., F.D., Z.S., and F.Z. conducted the experiments. W.G., T.Z., W.A., T.J., X.D., and C.B. wrote the manuscript. W.G, T.Z., W.A., T.J., C.B., and X.D. participated in the revision of the manuscript.

### Notes

The authors declare no competing financial interest.

## ACKNOWLEDGMENTS

This work was supported by the National Natural Science Foundation of China (81991505, 21534006, 82170928). We acknowledge the facilities and technical assistance provided by the Analytical Centre at Peking University Health Science Center.

## REFERENCES

(1) Levy, S. B.; Marshall, B. Antibacterial resistance worldwide: causes, challenges and responses. *Nat. Med.* **2004**, *10* (S12), S122−S129.

(2) D'Costa, V. M.; King, C. E.; Kalan, L.; Morar, M.; Sung, W. W.; Schwarz, C.; Froese, D.; Zazula, G.; Calmels, F.; Debruyne, R.; Golding, G. B.; Poinar, H. N.; Wright, G. D. Antibiotic resistance is ancient. *Nature* **2011**, *477* (7365), 457−461.

(3) Nizet, V.; Ohtake, T.; Lauth, X.; Trowbridge, J.; Rudisill, J.; Dorschner, R. A.; Pestonjamasp, V.; Piraino, J.; Huttner, K.; Gallo, R. L. Innate antimicrobial peptide protects the skin from invasive bacterial infection. *Nature* **2001**, *414* (6862), 454−457.

(4) Zasloff, M. Antimicrobial peptides of multicellular organisms. *Nature* **2002**, *415* (6870), 389−395.

(5) Gidalevitz, D.; Ishitsuka, Y.; Muresan, A. S.; Konovalov, O.; Waring, A. J.; Lehrer, R. I.; Lee, K. Y. Interaction of antimicrobial peptide protegrin with biomembranes. *Proc. Natl. Acad. Sci. U. S. A.* **2003**, *100* (11), 6302−6307.

(6) Zanetti, M. Cathelicidins, multifunctional peptides of the innate immunity. *J. Leukoc Biol.* **2004**, *75* (1), 39−48.

(7) Mukherjee, S.; Hooper, L. V. Antimicrobial defense of the intestine. *Immunity* **2015**, *42* (1), 28−39.

(8) Fjell, C. D.; Hiss, J. A.; Hancock, R. E.; Schneider, G. Designing antimicrobial peptides: form follows function. *Nat. Rev. Drug Discov* **2012**, *11* (1), 37−51.

(9) Erdem Buyukkiraz, M.; Kesmen, Z. Antimicrobial peptides (AMPs): A promising class of antimicrobial compounds. *J. Appl. Microbiol.* **2022**, *132* (3), 1573−1596.

(10) Linares, J. F.; Gustafsson, I.; Baquero, F.; Martinez, J. L. Antibiotics as intermicrobial signaling agents instead of weapons. *Proc. Natl. Acad. Sci. U. S. A.* **2006**, *103* (51), 19484−19489.

(11) Wright, G. D. The antibiotic resistome: the nexus of chemical and genetic diversity. *Nat. Rev. Microbiol* **2007**, *5* (3), 175−186.

(12) Martinez, J. L.; Baquero, F.; Andersson, D. I. Predicting antibiotic resistance. *Nat. Rev. Microbiol* **2007**, *5* (12), 958−965.

(13) Ferraboschi, P.; Ciceri, S.; Grisenti, P. Applications of Lysozyme, an Innate Immune Defense Factor, as an Alternative Antibiotic. *Antibiotics-Basel* **2021**, *10* (12), 1534.

(14) Bera, A.; Herbert, S.; Jakob, A.; Vollmer, W.; Gotz, F. Why are pathogenic staphylococci so lysozyme resistant? The peptidoglycan O-acetyltransferase OatA is the major determinant for lysozyme resistance of Staphylococcus aureus. *Mol. Microbiol.* **2005**, *55* (3), 778−787.

(15) Abouhmad, A.; Dishisha, T.; Amin, M. A.; Hatti-Kaul, R. Immobilization to Positively Charged Cellulose Nanocrystals Enhances the Antibacterial Activity and Stability of Hen Egg White and T4 Lysozyme. *Biomacromolecules* **2017**, *18* (5), 1600−1608.

(16) Ding, Y.; Shi, L.; Wei, H. Protein-directed approaches to functional nanomaterials: a case study of lysozyme. *J. Mater. Chem. B* **2014**, *2* (47), 8268−8291.

(17) Steiert, E.; Radi, L.; Fach, M.; Wich, P. R. Protein-Based Nanoparticles for the Delivery of Enzymes with Antibacterial Activity. *Macromol. Rapid Commun.* **2018**, *39* (14), e1800186.

(18) Phillips, D. C. The three-dimensional structure of an enzyme molecule. *Sci. Am.* **1966**, *215* (5), 78−90.

(19) Blake, C. C.; Koenig, D. F.; Mair, G. A.; North, A. C.; Phillips, D. C.; Sarma, V. R. Structure of hen egg-white lysozyme. A three-dimensional Fourier synthesis at 2 Angstrom resolution. *Nature* **1965**, *206* (4986), 757−761.

(20) Gilmore, J. M.; Scheck, R. A.; Esser-Kahn, A. P.; Joshi, N. S.; Francis, M. B. N-terminal protein modification through a biomimetic transamination reaction. *Angew. Chem., Int. Ed. Engl.* **2006**, *45* (32), 5307−5311.

(21) Scheck, R. A.; Dedeo, M. T.; Iavarone, A. T.; Francis, M. B. Optimization of a biomimetic transamination reaction. *J. Am. Chem. Soc.* **2008**, *130* (35), 11762−11770.

(22) Witus, L. S.; Moore, T.; Thuronyi, B. W.; Esser-Kahn, A. P.; Scheck, R. A.; Iavarone, A. T.; Francis, M. B. Identification of highly reactive sequences for PLP-mediated bioconjugation using a combinatorial peptide library. *J. Am. Chem. Soc.* **2010**, *132* (47), 16812−16817.

(23) Rosen, C. B.; Francis, M. B. Targeting the N terminus for site-selective protein modification. *Nat. Chem. Biol.* **2017**, *13* (7), 697−705.

(24) Gao, W.; Liu, W.; Mackay, J. A.; Zalutsky, M. R.; Toone, E. J.; Chilkoti, A. In situ growth of a stoichiometric PEG-like conjugate at a protein's N-terminus with significantly improved pharmacokinetics. *Proc. Natl. Acad. Sci. U. S. A.* **2009**, *106* (36), 15231−15236.

(25) Hao, H.; Sun, M.; Li, P.; Sun, J.; Liu, X.; Gao, W. In Situ Growth of a Cationic Polymer from the N-Terminus of Glucose Oxidase To Regulate H2O2 Generation for Cancer Starvation and H2O2 Therapy. *ACS Appl. Mater. Interfaces* **2019**, *11* (10), 9756−9762.

(26) Chiang, C. W.; Liu, X.; Sun, J.; Guo, J.; Tao, L.; Gao, W. Polymerization-Induced Coassembly of Enzyme-Polymer Conjugates into Comicelles with Tunable and Enhanced Cascade Activity. *Nano Lett.* **2020**, *20* (2), 1383−1387.

(27) Phillips, D. C. The Hen Egg-White Lysozyme Molecule. *Proc. Natl. Acad. Sci. U. S. A.* **1967**, *57* (3), 483−495.

(28) Sun, J.; Liu, X.; Guo, J.; Zhao, W.; Gao, W. Pyridine-2,6-dicarboxaldehyde-Enabled N-Terminal In Situ Growth of Polymer-Interferon alpha Conjugates with Significantly Improved Pharmacokinetics and In Vivo Bioactivity. *ACS Appl. Mater. Interfaces* **2021**, *13* (1), 88−96.

(29) Diamond, R. Real-space refinement of the structure of hen egg-white lysozyme. *J. Mol. Biol.* **1974**, *82* (3), 371−391.

(30) Pettersen, E. F.; Goddard, T. D.; Huang, C. C.; Meng, E. C.; Couch, G. S.; Croll, T. I.; Morris, J. H.; Ferrin, T. E. UCSF ChimeraX: Structure visualization for researchers, educators, and developers. *Protein Sci.* **2021**, *30* (1), 70−82.

(31) Konkolewicz, D.; Schroder, K.; Buback, J.; Bernhard, S.; Matyjaszewski, K. Visible Light and Sunlight Photoinduced ATRP with ppm of Cu Catalyst. *ACS Macro Lett.* **2012**, *1* (10), 1219−1223.

(32) Pan, X.; Malhotra, N.; Simakova, A.; Wang, Z.; Konkolewicz, D.; Matyjaszewski, K. Photoinduced Atom Transfer Radical Polymerization with ppm-Level Cu Catalyst by Visible Light in Aqueous Media. *J. Am. Chem. Soc.* **2015**, *137* (49), 15430−15433.

(33) Pan, X. C.; Tasdelen, M. A.; Laun, J.; Junkers, T.; Yagci, Y.; Matyjaszewski, K. Photomediated controlled radical polymerization. *Prog. Polym. Sci.* **2016**, *62*, 73−125.

(34) Corrigan, N.; Yeow, J.; Judzewitsch, P.; Xu, J.; Boyer, C. Seeing the Light: Advancing Materials Chemistry through Photopolymerization. *Angew. Chem., Int. Ed. Engl.* **2019**, *58* (16), 5170−5189.

(35) Parsons, S. M.; Raftery, M. A. The identification of aspartic acid residue 52 as being critical to lysozyme activity. *Biochemistry* **1969**, *8* (10), 4199−4205.

(36) Ko, J. H.; Maynard, H. D. A guide to maximizing the therapeutic potential of protein-polymer conjugates by rational design. *Chem. Soc. Rev.* **2018**, *47* (24), 8998−9014.

(37) Mansfield, K. M.; Maynard, H. D. Site-Specific Insulin-Trehalose Glycopolymer Conjugate by Grafting From Strategy Improves Bioactivity. *ACS Macro Lett.* **2018**, *7* (3), 324−329.

(38) Duan, F.; Jin, W.; Zhang, T.; Zhang, F.; Gong, L.; Liu, X.; Deng, X.; Gao, W. Self-Activated Cascade Biocatalysis of Glucose Oxidase-Polycation-Iron Nanoconjugates Augments Cancer Immunotherapy. *ACS Appl. Mater. Interfaces* **2022**, *14* (29), 32823−32835.

(39) Rawlinson, L. A.; Ryan, S. M.; Mantovani, G.; Syrett, J. A.; Haddleton, D. M.; Brayden, D. J. Antibacterial effects of poly(2-(dimethylamino ethyl)methacrylate) against selected gram-positive and gram-negative bacteria. *Biomacromolecules* **2010**, *11* (2), 443−453.

(40) Hudson, M. A.; Siegele, D. A.; Lockless, S. W. Use of a Fluorescence-Based Assay To Measure Escherichia coli Membrane Potential Changes in High Throughput. *Antimicrob. Agents Chemother.* **2020**, *64* (9), e00910−20.

(41) Nguyen, T. K.; Lam, S. J.; Ho, K. K.; Kumar, N.; Qiao, G. G.; Egan, S.; Boyer, C.; Wong, E. H. Rational Design of Single-Chain Polymeric Nanoparticles That Kill Planktonic and Biofilm Bacteria. *ACS Infect Dis* **2017**, *3* (3), 237−248.

(42) Mosaddad, S. A.; Tahmasebi, E.; Yazdanian, A.; Rezvani, M. B.; Seifalian, A.; Yazdanian, M.; Tebyanian, H. Oral microbial biofilms: an update. *Eur. J. Clin Microbiol Infect Dis* **2019**, *38* (11), 2005−2019.

(43) Deo, P. N.; Deshmukh, R. Oral microbiome: Unveiling the fundamentals. *J. Oral Maxillofac. Pathol.* **2019**, *23* (1), 122−128.

(44) Kilian, M.; Chapple, I. L.; Hannig, M.; Marsh, P. D.; Meuric, V.; Pedersen, A. M.; Tonetti, M. S.; Wade, W. G.; Zaura, E. The oral microbiome - an update for oral healthcare professionals. *Br Dent J.* **2016**, *221* (10), 657−666.

(45) Lynge Pedersen, A. M.; Belstrom, D. The role of natural salivary defences in maintaining a healthy oral microbiota. *J. Dent.* **2019**, *80* (Suppl 1), S3−S12.


https://doi.org/10.1021/acs.nanolett.2c03160
Nano Lett. 2022, 22, 8294−8303

(46) Sedghi, L.; DiMassa, V.; Harrington, A.; Lynch, S. V.; Kapila, Y. L. The oral microbiome: Role of key organisms and complex networks in oral health and disease. *Periodontol 2000* **2021**, *87* (1), 107−131.

(47) Lee, Y. H.; Chung, S. W.; Auh, Q. S.; Hong, S. J.; Lee, Y. A.; Jung, J.; Lee, G. J.; Park, H. J.; Shin, S. I.; Hong, J. Y. Progress in Oral Microbiome Related to Oral and Systemic Diseases: An Update. *Diagnostics (Basel)* **2021**, *11* (7), 1283.

(48) Lamont, R. J.; Hajishengallis, G. Polymicrobial synergy and dysbiosis in inflammatory disease. *Trends Mol. Med.* **2015**, *21* (3), 172−183.

(49) Hajishengallis, G.; Lamont, R. J. Beyond the red complex and into more complexity: the polymicrobial synergy and dysbiosis (PSD) model of periodontal disease etiology. *Mol. Oral Microbiol* **2012**, *27* (6), 409−419.

(50) Zhang, W.; Ju, J.; Rigney, T.; Tribble, G. Porphyromonas gingivalis infection increases osteoclastic bone resorption and osteoblastic bone formation in a periodontitis mouse model. *BMC Oral Health* **2014**, *14*, 89−89.

(51) Slots, J. Periodontitis: facts, fallacies and the future. *Periodontol 2000* **2017**, *75* (1), 7−23.

(52) Shi, B.; Chang, M.; Martin, J.; Mitreva, M.; Lux, R.; Klokkevold, P.; Sodergren, E.; Weinstock, G. M.; Haake, S. K.; Li, H. Dynamic changes in the subgingival microbiome and their potential for diagnosis and prognosis of periodontitis. *mBio* **2015**, *6* (1), e01926-14.

(53) Elashiry, M.; Morandini, A. C.; Cornelius Timothius, C. J.; Ghaly, M.; Cutler, C. W. Selective Antimicrobial Therapies for Periodontitis: Win the "Battle and the War". *Int. J. Mol. Sci.* **2021**, *22* (12), 6459.

## Recommended by ACS

**Peptide-Grafted Nontoxic Cyclodextrins and Nanoparticles against Bacteriophage Infections**

Łukasz Richter, Francesco Stellacci, *et al.*

OCTOBER 19, 2022
ACS NANO

READ

**Secondary Ammonium-Based Hyperbranched Poly(amidoamine) with Excellent Membrane-Active Property for Multidrug-Resistant Bacterial Infection**

Yunyun Xue, Baoku Zhu, *et al.*

JUNE 28, 2022
ACS APPLIED BIO MATERIALS

READ

**Onium- and Alkyl Amine-Decorated Protein Nanoparticles as Antimicrobial Agents and Carriers of Antibiotics to Promote Synergistic Antibacterial and Antibiofilm Activities**

Anjali Patel, Debasis Manna, *et al.*

NOVEMBER 11, 2022
ACS APPLIED NANO MATERIALS

READ

**Macrophage-Membrane-Camouflaged Nonviral Gene Vectors for the Treatment of Multidrug-Resistant Bacterial Sepsis**

Hongmei Cao, Jianfeng Liu, *et al.*

SEPTEMBER 28, 2022
NANO LETTERS

READ

**Get More Suggestions >**



https://doi.org/10.1021/acs.nanolett.2c03160
*Nano Lett.* 2022, 22, 8294−8303